PAPER

Mesoporous calcium silicate nanoparticles for superficial dental tissue reconstruction, *in vitro* and *in vivo*

Yixue Gao,[ab] Pin Huang,[b] Ruiying Chen,[b] Man Wang,[b] Yining Wang, [b][bc] Yue Sa*[bc] and Tao Jiang [b] *[bc]

The underlying dentin could be exposed to a humid atmosphere filled with bacteria if the covering enamel layer is broken because of external chemical and physical conditions. Accordingly, some diseases like bacterial invasion and dentin hypersensitivity often occur, which impact the daily life of patients. The study is aimed at evaluating the occluding effects of mesoporous calcium silicate nanoparticles (MCSNs) on the dentinal tubules *in vitro* and *in vivo*, as well as the antibacterial property and drug delivery ability when loaded with chlorhexidine (CHX) *in vitro*. MCSNs were synthesized according to the standard protocol. After a series of complimentary evaluations *in vitro* and *in vivo*, it was found that MCSNs and CHX–MCSNs could continually form apatite-like enamel layers on the exposed dentinal tubules and significantly reduced dentin permeability both *in vitro* and *in vivo*. Besides, MCSN and CHX–MCSN possessed low cytotoxicity *in vitro*, and only mild pulp inflammation was observed in two MCSNs containing groups *in vivo*. In addition, MCSN loaded with CHX released CHX sustainably and revealed a significant antibacterial effect against *E. faecalis in vitro*. Therefore, the results suggest that MCSN could be used as a promising biomaterial to occlude the dentinal tubules and carry antibiotics for avoiding further pulp infection.

1. Introduction

Enamel is a highly mineralized hard tissue covered on the surface of the tooth crown, of which mineralized structure takes up a larger proportion by weight (96%), and the remaining 4% comprises organic structure and plasma.[1,2] Dentin is the subject of tooth secreted by odontoblasts, protecting the inner pulp and supporting the outside enamel. The mineral phase of both enamel and dentin is hydroxyapatite (HA).[2,3] However, unlike enamel, dentin has a tubule structure. Dentinal tubules are arranged radially from the pulp to the enamel–dentinal junction, filling interstitial fluid and some odontoblastic process partially surrounded by nerve fibers.[3,4] For attrition, abrasion, caries, erosion, and other cases, dentin could be directly exposed to the oral environment caused by the overlying enamel loss.[5–7] As a result, external solutes, irritants, or bacteria may permeate through the dentinal tubules to the pulp, which will lead to the occurrence of many diseases associated with exposed dentin tubules.[4]

Dentin hypersensitivity (DH) features short or transient sharp pain due to the dentin being exposed to external chemical, tactile or thermal stimuli[8,9] and can cause patients to suffer extreme discomfort. It is reported that the prevalence of DH reaches 57% among adults; thus, it is a common clinical complaint of dental patients.[10–12] The hydrodynamic theory, proposed by Brannstrom *et al.*,[13] indicated that liquid movement in the dentinal tubules has a mechanical response to external stimuli. It flows from the inside to the outside when stimulated by the cold and is quite opposed when stimulated by the heat. Then the liquid flow stimulates a baroreceptor, generating a neural signal, which results in a painful sensation. As suggested by the theory, the potential effective treatment strategy of DH is to seal the dentinal tubules and block the external stimuli for preventing fluid flow, so as to relieve the clinical symptoms.[14] In addition, bacterial products, such as endotoxin, may diffuse across the open dentinal tubule toward the pulp and cause inflammatory reactions. Occluding dentinal tubules could also cut the passage of bacteria getting deeper into the pulp.[15,16] However, residual bacteria can survive for more than a year and can proliferate even in the presence of a good seal.[17] Consequently, if an adjunctive antibacterial drug could be effectively incorporated into the dentinal tubules-

[a]Department of Prosthodontics, The Affiliated Stomatological Hospital of Nanjing Medical University, Jiangsu Province Key Laboratory of Oral Diseases, Jiangsu Province Engineering Research Center of Stomatological Translational Medicine, PR China

[b]The State Key Laboratory Breeding Base of Basic Science of Stomatology (Hubei-MOST), Key Laboratory of Oral Biomedicine Ministry of Education, School & Hospital of Stomatology, Wuhan University, 237 Luoyu Road, Wuhan 430079, PR China. E-mail: jiangtao2006@whu.edu.cn; sayue@whu.edu.cn; Tel: +86 27 87686221

[c]Department of Prosthodontics, Hospital of Stomatology, Wuhan University, 237 Luoyu Road, Wuhan 430079, PR China

occluding agent, its local drug-delivering ability could prevent the detrimental effects from residual bacteria.

Calcium silicate (Ca-Si) features excellent degradability and bioactivity; therefore, it has been widely used as a potential bioactive material for the regeneration of bone tissue in the past twenty years.[18–20] Ca-Si based biomaterials could combine with the bone through chemical bonds, and a dissolution–precipitation reaction occurs at the interface to form an inorganic mineral similar to bone minerals, which is HA. However, studies have shown that HA deposition process as well as the bone-forming bioactivity could be influenced by the difference in the specific surface area (SSA) and microstructure of Ca-Si based materials.[21] Additionally, conventional Ca-Si based bioceramics do not have enough nano-pore structures, which restricts the ability to deliver drugs.[22,23] In order to improve these weaknesses, many attempts have been made to manufacture mesoporous nanostructured biomaterials and achieved great outcomes.[24–26] Li *et al.*[23] immersed the porous non-aggregated calcium silicate (MACS) in SBF for 4 h, and formed a hydroxyapatite mineral layer containing carbonate on the surface. Due to its high SSA and porosity, MACS exhibits stronger bone formation bioactivity than conventional amorphous calcium carbonate. Wei *et al.*[27] used mesoporous bioactive wollastonite as a filler for polycaprolactone. After immersing the composite in SBF for 1 week, a dense apatite layer was continuously observed on the surface. Since the conforming material has a high specific surface area and void ratio, the biological activity of the produced apatite is remarkably enhanced. Furthermore, such mesoporous Ca-Si materials exhibit a high loading capacity and an outstanding controlled release property. Therefore, they can also effectively load drugs as an underlying local drug-delivery system.[21,28] Xue *et al.*[29] indicated that mesoporous calcium–silica materials have a stronger adsorption capacity for lysozyme and bovine serum albumin than unmodified particles. According to sustained release kinetics results, the mesoporous calcium–silica material loaded with protein could continuously release for more than one week, while the unmodified particles just released within a few hours. Kang *et al.*[30] demonstrated that luminescent and mesoporous Eu^{3+}/Tb^{3+} doped calcium silicate microspheres obtained ibuprofen can be used to encapsulate drugs and release them. Since dentin and bones share a similar composition, it inspired us that Ca-Si materials and biomimetic approaches could effectively assist in the formation of an enamel-like mineral layer on the surface of dentin, thereby repairing the damaged biomineralized tissues in oral biology.[31–33] This idea, to the best of our knowledge, has not been described previously.

In view of the aforementioned, the present study is aimed at fully assessing the apatite formation ability, the occluding effects, biocompatibility, drug delivery ability, and antibacterial property exhibited by mesoporous Ca-Si nanoparticles (MCSN) on open dentinal tubules *in vitro* and *in vivo*. For this reason, MCSN was synthesized by a template route. Artificial saliva solution and rat incisors were designed to mimic the oral environment *in vitro* and *in vivo*, respectively. Additionally, the study selected the *Enterococcus faecalis* (*E. faecalis*), which is a bacteria usually

hiding in the dentin tubules,[34] as a bacterial model, and selected chlorhexidine (CHX), a kind of antibacterial agent with a broad spectrum for dental care,[35,36] as a drug model. $Ca(OH)_2$, a confirmed effective desensitizing material,[37] was used as the positive control group *in vivo*. The apatite formation ability and occluding effects of treatments *in vitro* were evaluated by Raman spectroscopy, attenuated total reflection infrared (ATR-IR) spectroscopy without destructiveness, scanning electron microscopy/energy dispersive spectrometer (SEM/EDS) observation, and permeability test. *In vivo* treatment effects were evaluated by SEM, hematoxylin–eosin (HE) staining, inflammatory score, and dentin permeability test.

2. Materials and methods

2.1 Material preparation

Calcium-silicate mesoporous nanomaterials (MCSN) were synthesized according to a template method.[34] Briefly, 6.6 g cetyltrimethylammonium bromide (CTAB) (Sigma-Aldrich, St. Louis, MO, USA) and 12 mL $NH_3 \cdot H_2O$ (Sinopharm Chemical Reagent Co. Ltd., Shanghai, China) were dissolved in 600 mL ddH_2O. 30 min of stirring was followed by the addition of 30 mL tetraethyl orthosilicate (TEOS) (Aladdin Industrial Corporation, Shanghai, China) together with 31.21 g $Ca(NO_3)_2 \cdot 4H_2O$ (Sinopharm Chemical Reagent Co. Ltd., Shanghai, China) with 3 h of vigorous stirring. After alternate filtering, the products were washed with ddH_2O and ethanol three times. Subsequently, collected powders underwent a drying process at 60 °C overnight together with 2 h of calcination at 550 °C for the removal of CTAB traces. The obtained MCSN was analyzed using scanning electron microscopy (S-4800, Hitachi), energy dispersive spectrometer (Hitachi), transmission electron microscopy (JEM-2100, JEOL, Tokyo, Japan), attenuated total reflection infrared spectroscopy (Nicolet, Madison, WI, USA), and X-ray diffraction (XRD, X′ Pert Pro, The Netherlands).

AS was used first to dilute the commercially available CHX solution (Sigma Chemical Co) to the final weight concentration of 2%, 0.2%, and 0.02% by AS. Then, 20 mg MCSNs were soaked into 2 mL of different concentrations of CHX–AS solution overnight at 4 °C for obtaining (0.02%, 0.2%, 2%) CHX-loaded MCSNs. After soaking, ethanol was used to wash the powders three times, which were then separated through 10 min of centrifugation at 10 000 rpm. Collected products received 6 h of drying processing at 60 °C.

2.2 *In vitro* dentin occlusion study

2.2.1 Sample preparation. The performance of all the experiments in the study followed related laws as well as institutional guidelines. The experimental protocol has been reviewed by and obtained the approval of the local Ethics Committee of the School and Hospital of Stomatology Wuhan University, China. After patients signed the informed consent, we obtained 40 caries-free extracted human third molars. All teeth were cleaned thoroughly and carefully examined under 20× magnification to ensure that they were free of fractures or caries and then stored in thymol (0.5%) at 4 °C for ≤30 days

before use. A 1.0 ± 0.1 mm thick dentin disk was cut from each tooth perpendicular to the long axis direction of the tooth above cemento-enamel junction using a low-speed diamond saw under water cooling (Isomet, Buehler, Lake Bluff, IL, USA). Every disc was prepared carefully and inspected cautiously to ensure no pulpal or coronal enamel exposure. Then, a 600-grit silicon carbide abrasive paper was used to polish the two sides of dentine specimens for 30 s irrigated by water constantly, aiming at creating a standard smear layer.

2.2.2 Design of experiments. Following material preparation, the smear layers of all dentin specimens were removed by 5 min of immersion into 0.5 M EDTA solution (pH 7.4) to open the dentinal tubules. Ultrasonic irrigation was applied to the etched disk, which was then preserved wet. After evaluating the original maximum permeability of each one as the baseline, dentine disks were randomly divided into 4 groups ($n = 10$):

(1) DW group: distilled water (DW) was used to brush dentin disks, which were then preserved in DW as a control.

(2) AS group: artificial saliva (AS) was used to brush dentin disks, which were then preserved in AS.

(3) MCSN–AS group: MCSN paste was used to slightly brush dentin disks for 1 min, which were then preserved in AS.

(4) 2%CHX–MCSN–AS group: 2%CHX-loaded MCSN paste was used to slightly brush dentin disks for 1 min, which were then preserved in AS.

The MCSN (2%CHX–MCSN) paste was obtained by mixing 0.1 g MCSN (2%CHX–MCSN) with 0.5 mL AS. The obtained MCSN (2%CHX–MCSN) paste was brushed on the dentin disks for 1 min using an electric toothbrush. After about 3 min of self-setting at room temperature, DW was used to rinse the residual MCSN (2%CHX–MCSN). Treated specimens were placed in 50 mL AS or DW at 37 °C for seven days, and the fresh solutions were changed every 24 h. After 7 days of immersion, the samples received 1 min of treatment with 6% citric acid (pH 1.5) for simulating the acid challenge in an oral environment. The compositions of the AS were 50 mmol L^{-1} KCl, 1.5 mmol L^{-1} CaCl$_2$, 20 mmol L^{-1} Tris, and 0.9 mmol L^{-1} KH$_2$PO$_4$, and pH was adjusted to 7.4.

2.2.3 ATR-IR spectroscopy detection. After EDTA etching and 1 day, 3 day, and 7 day storage as well as the acid challenge, ATR-IR spectra were acquired using a Nicolet 5700 FTIR spectrophotometer (Nicolet, Madison, WI, USA) with a diamond crystal ATR accessory as the internal reflection element. The reference point was marked on each specimen's back surface for analyzing the real-time dentin disk change at the same position prior to and after the treatment. Then we collected spectra in the range of 800–1800 cm^{-1} under 4 cm^{-1} resolution with 64 scans. The OMNIC 8 software helped to analyze the obtained ATR-IR. The average value of every specimen was analyzed at three different sites prior to and after the treatments. After water subtraction, baseline correction, and normalization to the Amide I peak, the mineral matrix ratio, *i.e.*, the ratio of integrated areas of the phosphate ν_1, ν_3 contour to the Amide I peak, M : M, was measured before and after the treatment for quantitatively calculating the mineral change extent.

2.2.4 Raman spectroscopy detection. Raman spectra were obtained based on the identical three dentin specimens in each group after EDTA etching, after 1 day, 3 day, and 7 day storage and acid challenge by micro-Raman spectroscopy (i-Raman Portable Raman Spectrometer, B&W TEK Inc., USA) together with a semiconductor laser diode at 785 nm wavelength. The reference point was marked for every specimen for analyzing at the same position prior to and after the treatment, in the range of 0–3200 cm^{-1} and an integration time of 20 000 m s^{-1} at room temperature. BWSpec 4 spectroscopic software (BWSpec, B&W TEK Inc.) was employed to visualize and process the acquired spectral data. Original spectra underwent baseline correction and then smoothed to avoid the fluorescence of the laser. All these values were represented by percentages.

2.2.5 SEM/EDS detection. SEM helped to observe the surface morphology of dentin discs after 1 week treatment together with the subsequent acid challenge. Samples were dried in a desiccator and coated with gold in a vacuum evaporator (E1010, Hitachi, Japan), then a field emission SEM (S-4800, Hitachi, Japan) was used to observe them at 10 kV. An energy-dispersive X-ray spectrometer (Hitachi) attached to the SEM was used to obtain the EDS results. Each sample was analyzed three counts at 20 kV, the working distance was 10–15 mm, and the counting time was 130 s.

2.2.6 Dentine permeability evaluation. According to our previous studies, dentin permeability was tested using a special liquid filtration device in a modified split-chamber unit that simulates the pressure of the pulp chamber with a 20 cm water column. A pair of rubber "O" rings were used to tightly fix each dentine disk (each ring is connected to a 2 cm × 2 cm × 0.5 cm plexiglass slab) for filtering deionised water. Ten samples were evaluated in each group. The initial value after EDTA treatment was set as the baseline (100%), and each sample was re-measured after 7 days of different treatments and acid challenge. The permeability possessed by each specimen was represented as Lp% compared with the EDTA-etched value of the same specimen.

2.3 *In vitro* antibiotics release test

The UV analysis was carried out to determine the loading amount and sustained release of CHX at a wavelength of 254 nm, relying on the calculation of the concentration before and after the different periods. MCSN powder loaded with different CHX concentrations was soaked into a specific amount of fresh AS (50 mL) at 37 °C for the complete reaction. 2 mL solution was taken out each time for testing, and 2 mL fresh AS was re-added, followed by calculating the accumulative percentage of the CHX released from the MCSN disc.

2.4 *In vitro* antibacterial test

For investigating the antibacterial action of MCSN and drug-loaded MCSN, the disk-diffusion method was used against *E. faecalis*. 30 μL of *E. faecalis* suspensions with a concentration of 0.05–2 mg mL^{-1} was dropped onto the Petri dishes, which contained brain heart infusion broth culture medium, followed by a uniform distribution. After MCSN and CHX were fully reacted, a syringe was used to inject the mixture into a mold

with a diameter of 13.0 mm and height of 0.5 mm to form a drug-loaded sample required for the experiment. Then, the pieces were placed on the center of the semi-solid medium and cultured in a 37 °C incubator for 24 h. Three samples in each group were repeatedly tested three times. After that, the zone of inhibition (ZOI), the clear region near the disc that was saturated with an antimicrobial agent on the surface of agar, was measured and averaged.

2.5 *In vitro* cell culture and cytotoxicity assay

After the patient's informed consent, premolars extracted for orthodontic treatment were collected, with human dental pulp cells (HDPCs) isolated from the healthy human dental pulp tissues. The obtained pulp tissues were harvested and cultured *in vitro* under the protocol, and the third generation dental pulp cells were applied. *In vitro* cytotoxicity of MCSN and 2%CHX–MCSN were measured according to the Cell Counting Kit-8 (CCK-8) reagent instructions (Dojindo Molecular Technologies, Kumamoto, Japan). The HDPCs were seeded in 96-well plates at a density of 5000 cells per well, followed by 24 h of incubation with 5% CO_2 at 37 °C. A concentration gradient of $Ca(OH)_2$, MCSN, and 2%CHX–MCSN (0, 10, 20, 40, 80, 160, 320, and 640 mg mL^{-1}) was added to the cell plate for another 24 h. Subsequently, 10 mL of CCK-8 solution was added to each well together with 2 h of incubation. The microplate reader (PowerWave XS2, BioTek Instruments Inc., Winooski, VT, USA) was used to monitor the optimal density at 450 nm. We expressed these results as the relative cell viability (%) in comparison with a control group containing only the culture medium. The experiment was carried out repeatedly 6 times.

2.6 *In vivo* study

2.6.1 Surgical procedure. All animal procedures were performed in accordance with the Guidelines for Care and Use of Laboratory Animals of Wuhan University and approved by the Animal Ethics Committee of the School and Hospital of Stomatology Wuhan University, China. Forty 2–3 months old male rats (Rattusnorvegicus; Wistar), weighing 200–300 g, offered 160 teeth for the study (upper incisor and lower incisor). The desensitizing agents helped to randomly divide these animals into 4 groups ($n = 10$ rats per group, 40 teeth per group):

(1) DW group: teeth were brushed with distilled water (control);

(2) $Ca(OH)_2$ group: teeth were brushed with $Ca(OH)_2$;

(3) MCSN group: teeth were brushed with MCSN paste;

(4) 2%CHX–MCSN group: teeth were brushed with 2%CHX-loaded MCSN paste.

After intraperitoneal injection of anesthesia (75 mg kg^{-1} ketamine together with 10 mg kg^{-1} xylazine), cavities with a depth of 0.3 mm and a width of 0.8 mm were prepared at the cervical region on the buccal surface in the upper incisor and lower incisor relying on a standard (active tip with 0.3 mm) #245 carbide bur (S.S. White, Rio de Janeiro, Brazil). Before processing different materials, all the dentin cavities were treated with tiny cotton pellets with 24% EDTA gel. The cavities were covered for

3 min for the removal of the smear layer and the opening of the dentinal tubules. The cotton pellet was replaced every 30 s.

Experimental agents were adopted to brush the teeth with the help of the toothbrush for children (Colgate Kids). Fifteen toothbrushing movements were applied, and the force for toothbrushing was applied by the same laboratory staff once daily for 4 days. Before the experiment ended, the rats were sacrificed as required, and the upper and lower incisors were carefully extracted.

2.6.2 Dentin permeability. After each daily treatment, a pipette was used to dispense 5 μL of 5% Evans blue dye at each cavity for 5 min for the fuel to penetrate into the dentin tubules to observe the dentin permeability change.

2.6.3 SEM detection. The morphology of the sample surfaces after 4 day treatment in each experimental group was observed by SEM. A water-cooled diamond saw was used for transverse specimen sections. The sectioned specimens were ultrasonicated for 10 min with 20 mL DW. The samples were dewatered using a concentration gradient of ethanol for 10 min (namely 25%, 50%, 70%, 90%, or 100%) and dried. The dried specimens were placed on the metal stub in a 37 °C incubator for one day and in a vacuum silica gel desiccator for two days. Finally, 25 nm of gold was used to sputter-coat these samples for 100 s to perform the SEM analysis.

2.6.4 Pulp irritation assay. In terms of the irritation test about dental pulp, Hematoxylin & Eosin (H&E) stain was adopted for the histological analysis after preparing other parts of separated specimens. A light microscope was used to evaluate the intensity exhibited by the pulp response. Heyeraas *et al.*[39] have categorized the pulp inflammation into four degrees as follows:

• Score 0 (none): normal pulpal tissue;

• Score 1 (mild): there is a small number of inflammatory cells and extravasated red blood cells;

• Score 2 (moderate): mononuclear and neutrophilic leukocytes are likely to invade the odontoblast–predentin area (it is impossible to identify the normal pseudostratified appearance of these odontoblasts);

• Score 3 (severe): the marked cellular infiltration, such as abscess formation. Polymorphonuclear and mononuclear leukocytes dominated the affected area.

2.7 Statistical analysis

SPSS 19.0 (SPSS, Chicago, IL, USA) was applied to the statistical analyses for WINDOWS. The two-way repeated-measures analysis of variance (RMANOVA) was used to analyze the overall treatment effect, taking treatment and treatment time as the main effect and repeated measure, respectively. One-way ANOVA together with a *post hoc* Tukey test assisted in analyzing the *in vivo* dentin permeability results and the ZOI values. The significance level was set at 0.05 for the *P* value.

3. Results

3.1 Material characterization

A facile chemical precipitation approach helped to successfully synthesize the MCSN using CTAB as the template. From SEM
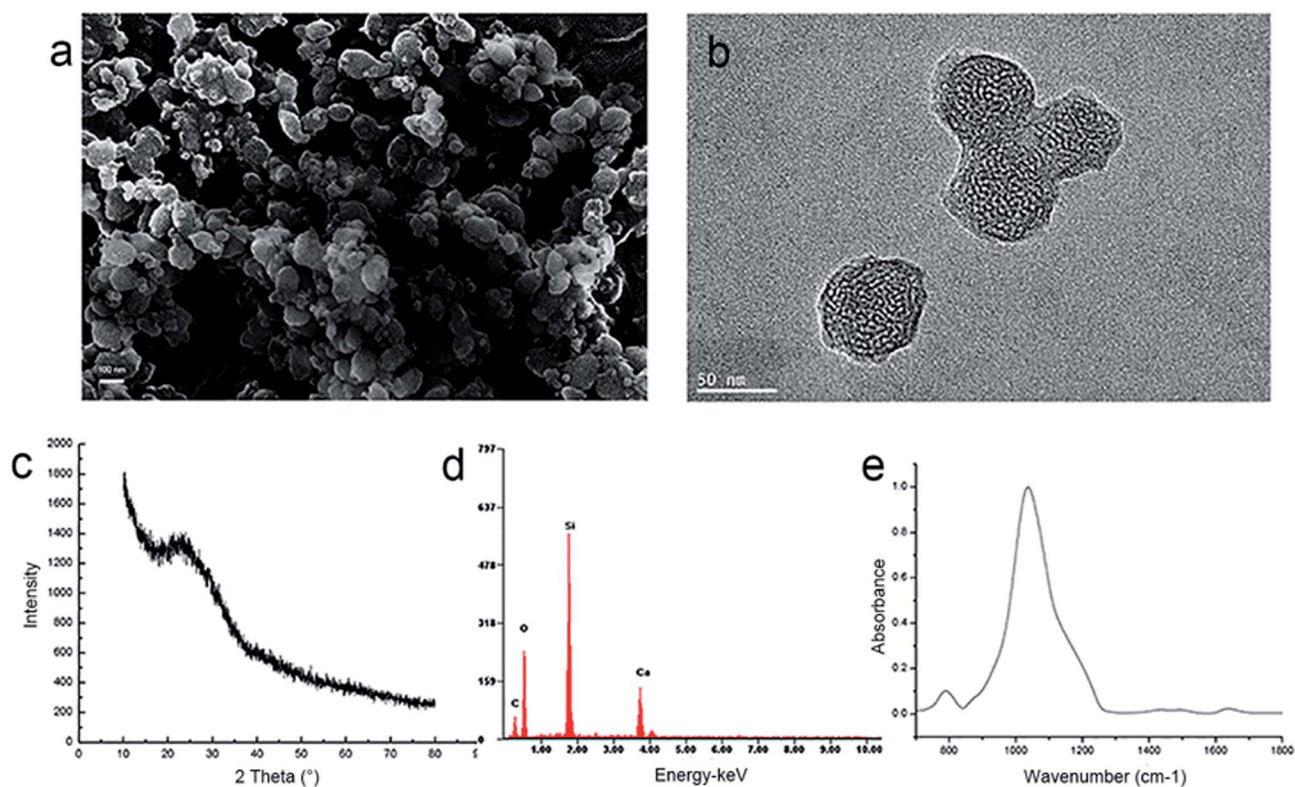
Fig. 1   Characterization of MCSN using SEM (a), TEM (b), XRD (c), EDS (d), and ATR-IR (e).
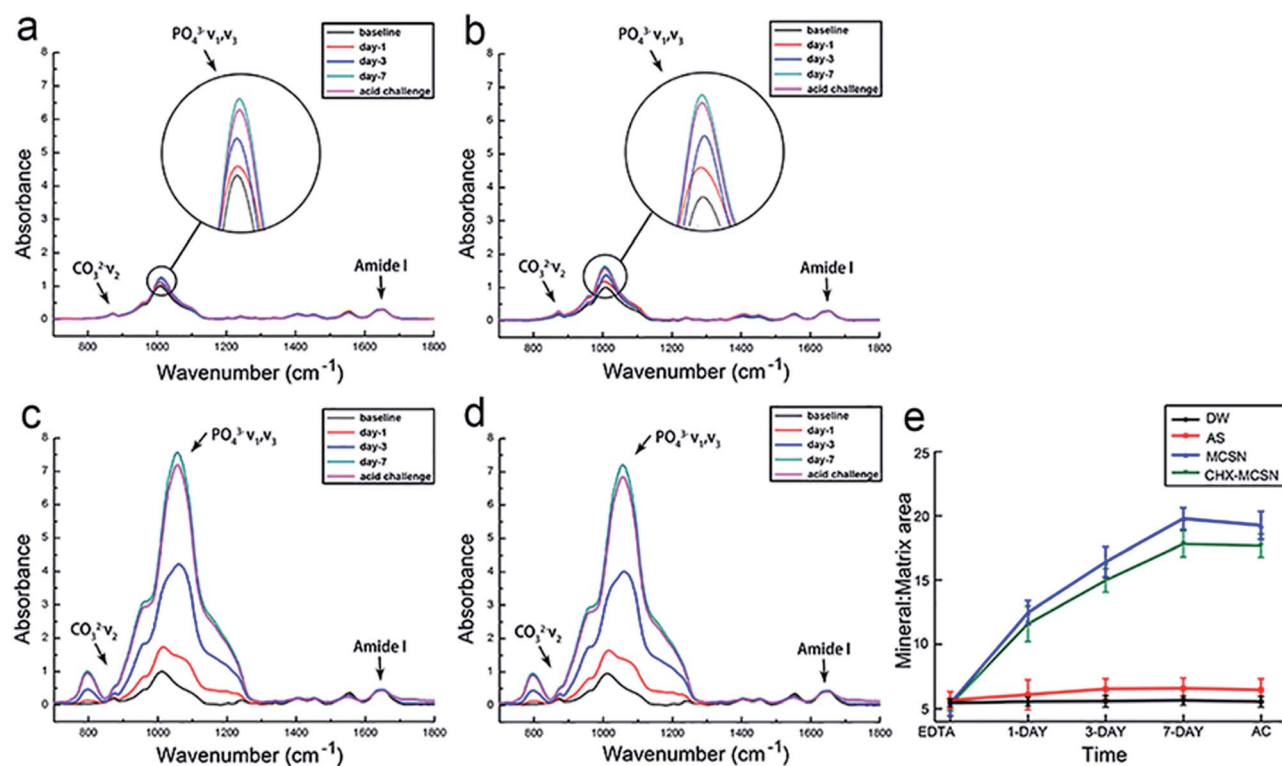

Fig. 2   Representative ATR-IR spectra (a–d) of dentin surface remineralization marked in different colors at different time points. (a) DW group; (b) AS group; (c) MCSN–AS group; (d) 2%CHX–MCSN–AS group. (e) The mineral matrix area ratio after different time points for each group (the data represented as mean and standard deviations).

analysis, the MCSN particles are nearly 100 nm in size (Fig. 1a). TEM showed that the particles possess an internal nano-porous structure (Fig. 1b). As found in the XRD result, MCSN is amorphous (Fig. 1c). From the EDS results, the main elements of MCSN were calcium, silicon, carbon, and oxygen (Fig. 1d). ATR-IR spectra showed two prominent peaks of MCSN at about 700–1300 cm^{-1} (Fig. 1e).

3.2 *In vitro* dentin occlusion study

3.2.1 ATR-IR spectroscopy. The spectra in the region of 800–1800 cm^{-1} were intercepted as a representative record. The band at 885–1180 cm^{-1} is assigned to v_1, v_3 PO$_4^{3-}$, representing mineral components, and the band from 1600 to 1725 cm^{-1} is assigned to Amide I, representing organic components. In MCSN–AS and 2%CHX–MCSN–AS groups, there was an obvious uptrend for the v_1, v_3 PO$_4^{3-}$ peak in the 7 day immersion, while v_1, v_3 PO$_4^{3-}$ peak changed slightly in the DW group and AS group in the 7 day immersion (Fig. 2a–d). Both treatment and time and their interactions had significant effects on mineral matrix area ratio (MM ratio) illustrated by Tukey's multiple comparison tests and two-way RMANOVA ($p < 0.001$). Specifically, the MM ratio increased significantly from 5.48 up to 20.13 for the MCSN–AS group and from 5.37 to 17.88 for the 2%CHX–MCSN–AS after 7 day AS immersion ($p < 0.001$). Comparatively, after 7 day immersion, the MM ratio of the DW group or AS group did not change at all ($p > 0.05$) (Fig. 2e). There was an apparent increase in the v_1, v_3 PO$_4^{3-}$ peak of MCSN–AS group and 2%CHX–MCSN–AS group compared with the DW group or AS group after 7 day immersion. DW and AS groups showed no noticeable difference after 7 day immersion. After 1 min of acid challenge, the MM ratio did not change greatly in any group ($p > 0.05$).

3.2.2 Raman spectroscopy. Fig. 3 displays the major features possessed by the Raman scattering spectra. The highest peak observed at 960 cm^{-1} is assigned to v_1 PO$_4^{3-}$. The peaks at 1045 cm^{-1} and 1024 cm^{-1} are attributed to v_3 PO$_4^{3-}$. The classic peak at 1068 cm^{-1} is caused by v_3 CO$_3^{2-}$. Based on the two-way RMANOVA analysis, the major effect on the v_1 PO$_4^{3-}$ value intensity for both treatment and time as well as the interaction between them is of statistical significance ($p < 0.001$). The v_1 PO$_4^{3-}$ intensity increased significantly in the MCSN–AS group and 2%CHX–MCSN–AS group after 7 day AS immersion ($p < 0.001$), whereas it showed no noticeable change in the other two groups ($p > 0.05$). After 1 min of acid challenge, the v_1 PO$_4^{3-}$ intensity showed no significance in any group ($p > 0.05$) (Fig. 3a–e).

3.2.3 SEM/EDS analysis. As can be seen from the pictures in the DW group, after 7 day treatment, there is no smear layer in the dentine surfaces, and dentinal tubules were clearly visible. The number of mineral-like deposits was small on the surface of dentin in the AS group. However, in the MCSN–AS group and 2%CHX–MCSN–AS groups, dentin surfaces were
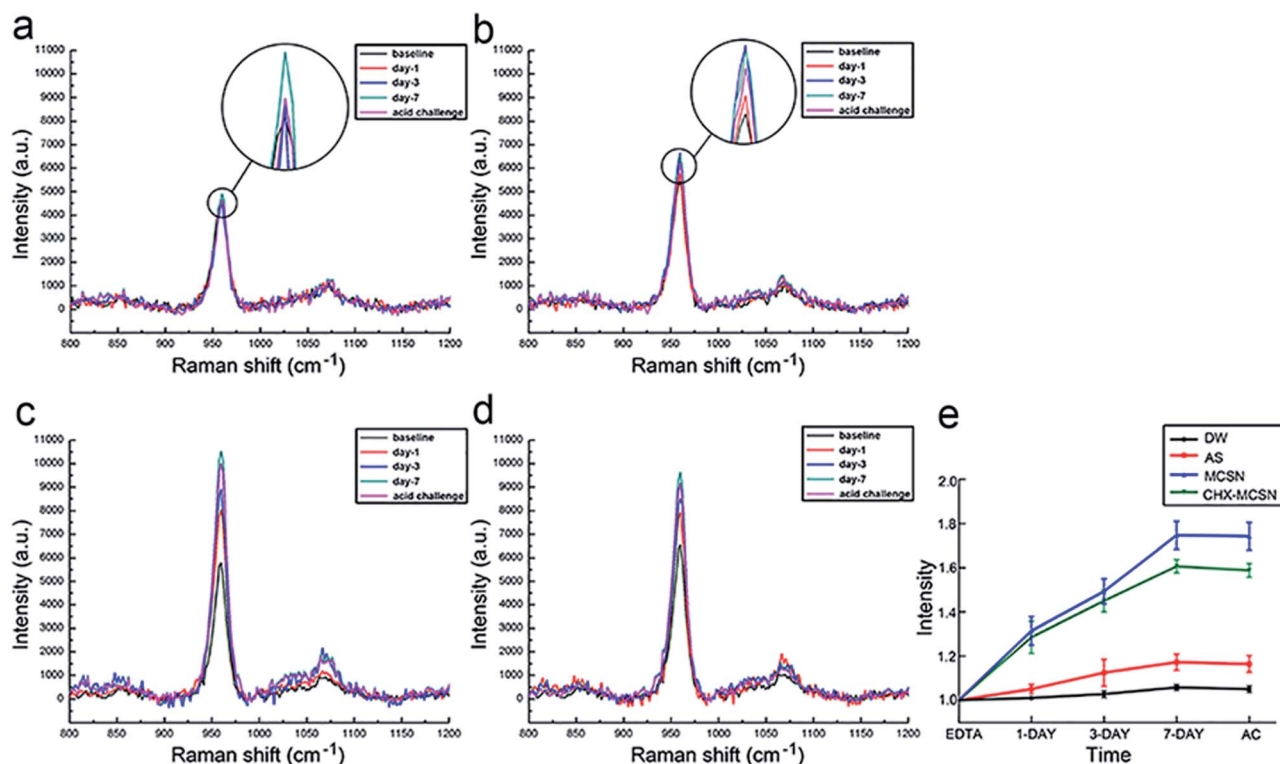

Fig. 3 Raman spectra of dentin surface remineralization marked in different colors at different time points. (a) DW group; (b) AS group; (c) MCSN–AS group; (d) 2%CHX–MCSN–AS group. (e) The ratio of intensity values of v_1 PO$_4^{3-}$ peak were recorded where the baseline ratio was set at 1.0, and the ratio that has been changed afterward was calculated as a relative ratio of the baseline (the data represented as mean and standard deviations).
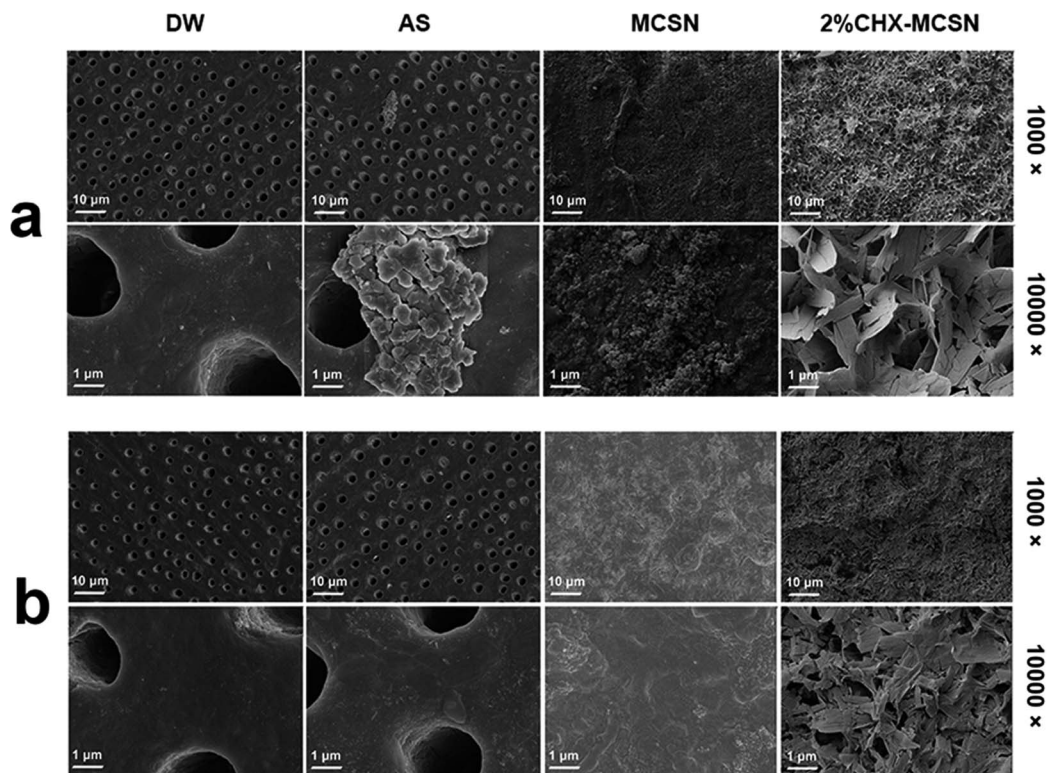
© 2021 The Author(s). Published by the Royal Society of Chemistry

Fig. 4 Dentin surface morphology by different treatments (a) after 7 day immersion; (b) after acid challenge.

almost covered by a layer of crystal-like deposits (Fig. 4a). After the acid challenge, open dentine tubules were completely exposed on dentine surfaces in DW and AS groups. By contrast, the apatite layers left on the dentin disk surface were relatively flat in the MCSN–AS group and 2%CHX–MCSN–AS groups, which still can assist in effectively occluding the dentinal tubules (Fig. 4b). Fig. 5 displays the EDS results. The main elements in DW and AS groups include carbon, phosphorus, oxygen, and calcium. The silicon levels are significantly higher in the MCSN–AS group and higher chlorine level but lower silicon level in the 2%CHX–MCSN–AS group, including the presence of calcium, phosphorus, carbon, and oxygen. After the
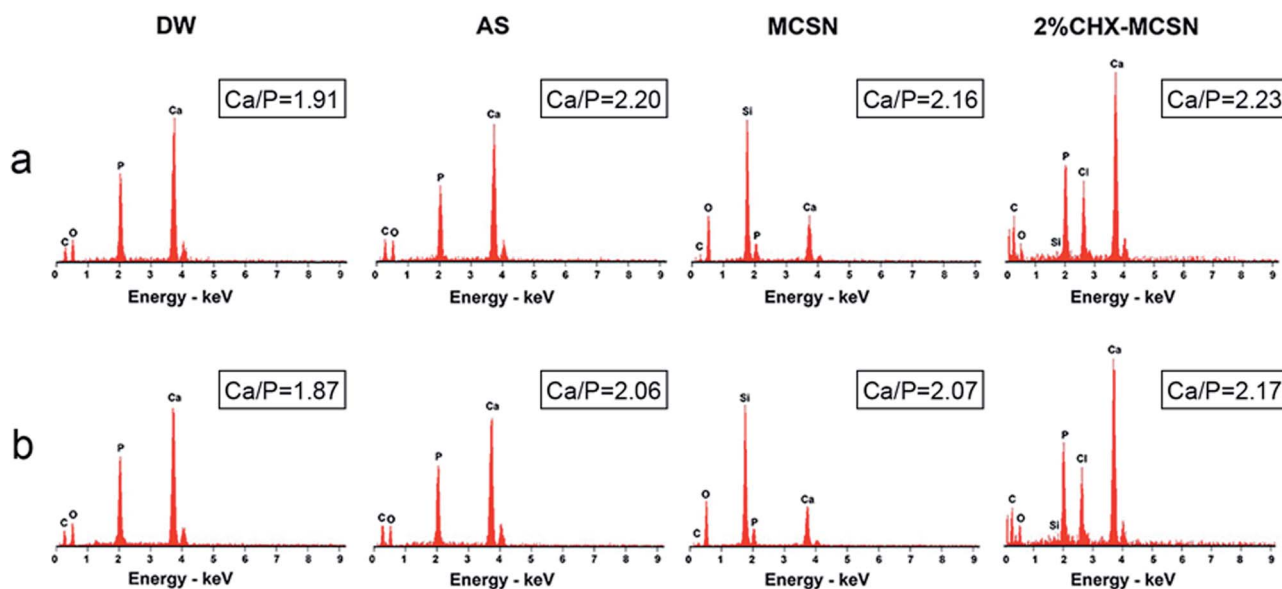

Fig. 5 EDS analysis of dentin surface after 7 day immersion (a) and acid challenge (b).

acid challenge, there was no significant change in any of the groups.

3.2.4 Measurement of dentine permeability. The initial dentine permeability is set as the percentage of the largest permeability (100%) following EDTA etching. The dentine permeability data under 4 different treatments are shown in Table 1. As demonstrated by statistical analysis, dentine permeability reduced remarkably in the MCSN–AS group ($p <$ 0.001) and 2% CHX–MCSN–AS group ($p < 0.001$), while neither AS immersion ($p > 0.05$) and DW immersion ($p > 0.05$) could significantly affect the dentine permeability after treatments. After the acid challenge, there is an increase in the dentine permeability exhibited by all four groups. Statistical significance was observed only in the AS group ($p = 0.026$). No significance was found in DW, MCSN–AS, and 2%CHX–MCSN–AS groups by citric acid treatment ($p > 0.05$).

3.3 *In vitro* antibiotic release

The drug-loaded MCSN can release CHX continuously in AS for a long time (Fig. 6). The cumulative percentage of the final release showed no significant difference regarding the loading efficiency exhibited by MCSN powder loaded with three CHX concentrations (namely, 0.02%, 0.2%, and 2%) ($p > 0.05$). For all of them, the CHX loading efficiency was high at about 75% even after 1 week, demonstrating good drug loading and sustained release properties of MCSN.

3.4 *In vitro* antibacterial property

According to the analysis results of the inhibition and antibacterial ability exhibited by CHX-loaded MCSN, all measured plates presented a translucent zone against the *E. faecalis* (Fig. 7). The diameter of ZOI enlarges with the increase in the CHX in MCSN concentration. These groups show a statistical significance ($p < 0.001$).

3.5 *In vitro* cytotoxicity assay

Fig. 8 displays the relative cell viability possessed by HDPCs with exposure to various concentrations of Ca(OH)$_2$, MCSN, and 2%CHX–MCSN (0–640 mg mL^{-1}). MCSN group presents no obvious difference ($p > 0.05$). An obvious difference was observed between certain concentrations of 80 mg mL^{-1} and 160 mg mL^{-1} in the Ca(OH)$_2$ group ($p < 0.05$) and 160 mg mL^{-1} and 320 mg mL^{-1} in the 2%CHX–MCSN group ($p < 0.05$).
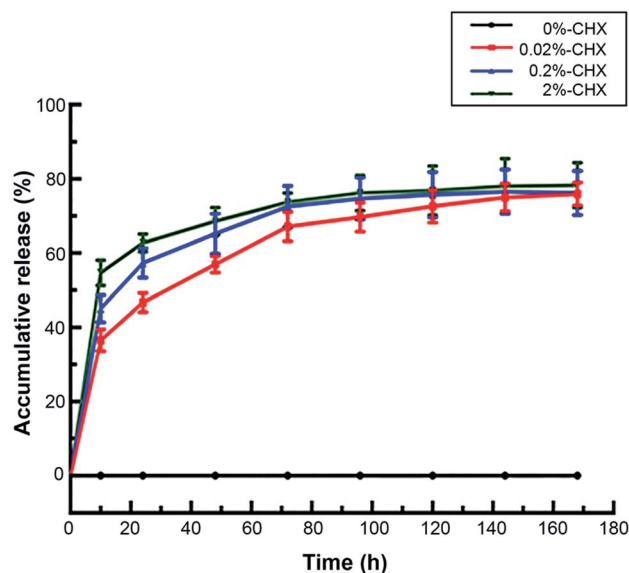

Fig. 6 Accumulative release of CHX from the MCSN with different concentrations over a week time (the data represented means and standard deviations).

3.6 *In vivo* study

3.6.1 Dentin permeability. Fig. 9 shows the mean and SDs of dentin permeability to the 5% Evans blue dye. There was a noticeable difference in Ca(OH)$_2$, MCSN–AS, and 2%CHX–MCSN–AS groups compared with the DW group ($p < 0.001$). No obvious difference was found between the MCSN–AS group and the 2%CHX–MCSN–AS group ($p > 0.05$).

3.6.2 SEM observation. After 4 days of treatment, the dentinal tubules in the DW group are open, and almost all of the surfaces do not have a smear layer. Most dentin tubules were occluded by deposits, while only a few tubules were open in the Ca(OH)$_2$ group. However, in the MCSN group and 2% CHX–MCSN group, it is found that the crystal-like deposit layer occluded nearly all the dentinal tubules (Fig. 10).

3.6.3 Pulp irritation assay. Fig. 11 shows representative histological analyses of different groups after 4 days of treatment. In the Ca(OH)$_2$ group, the blood vessels were full of erythrocytes, implying congestion. Specific to the MCSN and 2% CHX–MCSN groups, only mild pulp inflammation was observed. Unexpectedly, a more obvious odontoblast layer was observed in the pulp tissue in the 2%CHX–MCSN group. The percentages of inflammatory scores of different groups are

Table 1 Permeability following treatments^a

Treatments	No treatment	DW	AS	MCSN	2%CHX–MCSN
EDTA application	100 ± 0	100 ± 0	100 ± 0	100 ± 0	100 ± 0
7 day treatment	100.2 ± 3.1	99.7 ± 3.8	93.7 ± 6.2	23.0 ± 10.6	31.0 ± 9.4
Acid challenge	102.8 ± 7.2	101.1 ± 5.1	96.9 ± 10.3	28.2 ± 13.9	34.6 ± 11.7

^{a} The values (%) are expressed as means $\pm$ standard deviations. Lp following the EDTA treatment corresponds to the largest permeability (Lp = 100%).
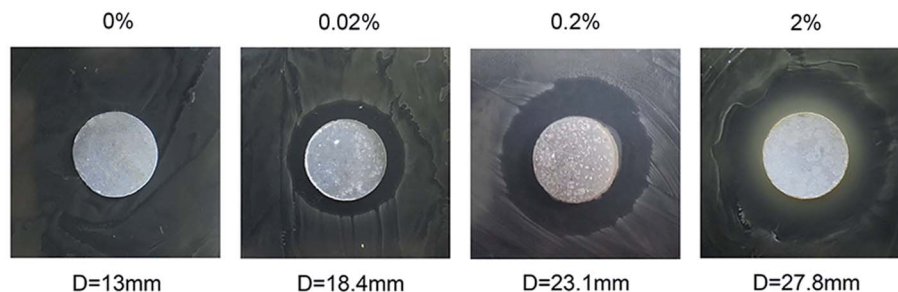
Fig. 7 Antibacterial activity of disc-like samples by the zone of inhibition (ZOI) test against *E. faecalis*.
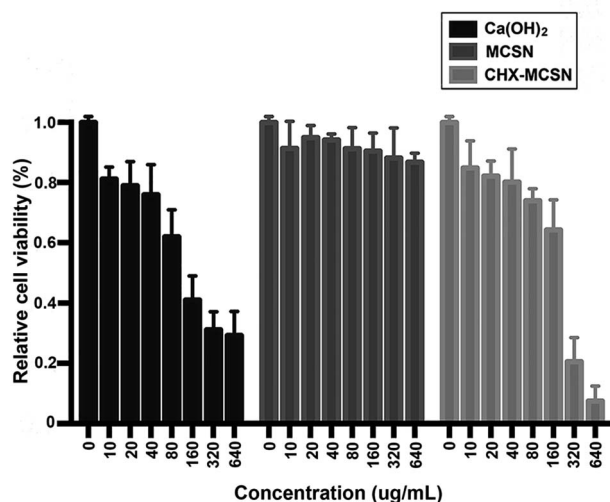

Fig. 8 Relative cell viability of HDPCs exposed to different concentrations ($0-640$ mg mL^{-1}) of Ca(OH)$_2$, MCSN, and CHX–MCSN for 24 h. Results are shown as mean $\pm$ S.D.

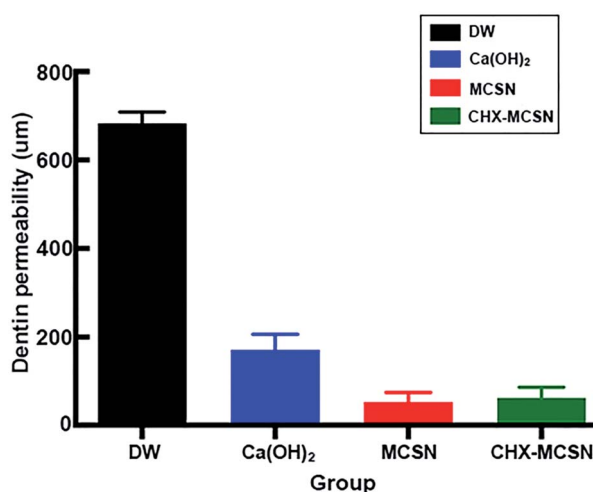presented in Fig. 12. Statistical significances were found in the inflammatory scores between DW and two MCSN containing groups ($p < 0.05$). No difference was found between the DW group and the Ca(OH)$_2$ group ($p > 0.05$).

Fig. 9 Mean and standard error of dentin permeability (5% Evans blue dye) after different treatments.

4. Discussion

Here, the MCSN was successfully manufactured, and the CHX was efficiently loaded into MCSNs using a mixing–coupling method. In the procedure of MCSN manufacture, the Si (TEOS) and the metal elements (such as Ca in Ca(NO$_3$)$_2$) took chemical interactions and combination through a template (CTAB) to form the mesoporous skeleton.[38] It is easy to prepare the MCSN nanoparticles as an injectable paste for filling the tooth defect, which could avoid dental structure being excessively cut for the reconstruction of the damaged enamel by adopting minimum intervention therapy in future clinical applications. Further, MCSN possesses a larger surface area and higher pore volume,[22,38] showing beneficial effects on delivering antibiotics for antibacterial effects.

Mineralization abilities of MCSN and CHX–MCSN were observed in both qualitative and quantitative ways. ATR-IR and Raman spectroscopy approaches contribute to the quantitative characterization of the forming ability exhibited by the mineral in real-time.[7,40,41] In the *in vitro* study, the MM ratio from the ATR-IR spectra and the intensity exhibited by v_1 PO$_4^{3-}$ from Raman spectra did not change in DW and AS groups after 7 days of treatment. However, they increased dramatically in the two MCSN contained groups, which directly confirmed that the apatite crystals were continuously formed on the dentin surface. SEM examinations supported the molecular evidence from ATR-IR and Raman spectra in a qualitative way. The control group showed open tubules, and the two MCSN containing groups showed crystal deposit layer obstructing dentin tubules excellently. However, the morphologies of these two layers were different. This result further confirmed the apatite-forming ability of MCSN on dentin surface and also indicated CHX may combine with MCSN and interfere with the transformation of MCSN products without affecting the occluding effect of MCSN. Previous research[42] suggested that the abundant active functional groups in MCSNs could bind with those in CHX *via* a covalent binding process. During this period, the CHX could be linked onto the Si^{4+} skeleton of mesoporous structures to form the final apatite products.

To further investigate the stability of the mineralization product, citric acid was used to simulate the oral environment because it commonly constitutes soft drinks and fruit.[40,41] After the acid challenge, all groups showed no significant changes in mineral matrix from ATR results, no significant decrease in v_1
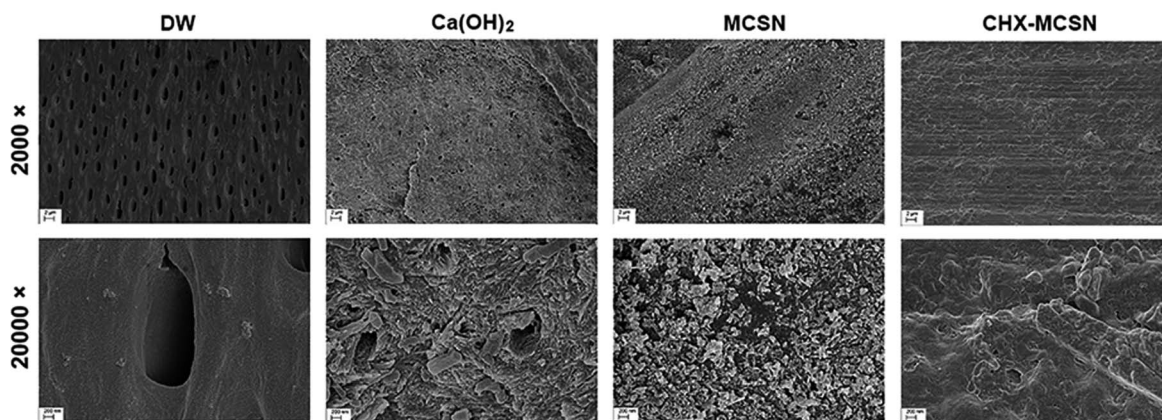
Fig. 10 SEM photomicrographs of dentin surface after different treatments.
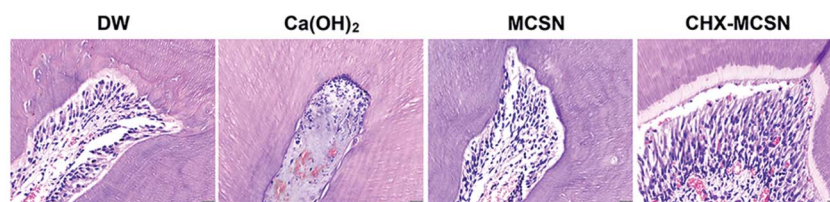

Fig. 11 Histological analysis (H&E stain) of pulp tissue in the animal study.

PO_4^{3-} intensity from Raman results, and no significant alteration of element type from EDS results, respectively. SEM result complementarily revealed the morphological details after exposure to the acid environment. After treating with citric acid for 1 min, no obvious change was observed in the DW group, and the mineral-like deposits in AS group disappeared. But in contrast, the surface morphologies of the formed crystal layer became denser and flatter in the two MCSN containing groups, and all dentin tubules were still blocked well. These results together proved that the acid could only remove the superficial products without dissolving the underlying minerals. Further, the MSCN-induced minerals could finally form a dense and enamel-like layer to protect the underlying dentin. Although

a previous study also proved the CHX could bind to phosphate groups acting as a co-surfactant on the etched surface to increase the surface free energy and create an acid-resistant layer,[17] the exact chemical mechanism behind the combination of MCSN and CHX still needs further investigation.

In vivo SEM results displayed a similar phenomenon as the *in vitro* study, which showed open tubules in the control group but crystal deposit layer in the other three groups. Further comparisons within the three groups showed that a few open tubules could still be seen in the Ca(OH)$_2$ group while the formed apatite had fully filled the dentin tubules in the two MCSN containing groups. These phenomena directly proved the *in vivo* occluding ability of MCSN products on dentinal tubules and clearly revealed the stability of these enamel-like mineral layers by continuous saliva flow, mastication, deglutition, and bruxism of rats *in vivo*.

Dentin permeability results supported the SEM findings in our study. No significant change of Lp% in DW and AS groups were observed but significantly reduced Lp% was found in MCSN and CHX–MCSN groups after 7 days of treatment *in vitro*. These results were consistent with the SEM result that products from MCSN and CHX–MCSN showed an excellent occluding effect on dentin surfaces after 7 day immersion. After the acid challenge, only Lp% of AS group increased, indicating that AS-induced crystals did not stick to the dentin surface firmly in comparison with MCSN and 2%CHX–MCSN-induced crystals *in vitro*. *In vivo* dentine permeability result showed consistency with the *in vitro* result. The blue dye analysis, which reproduced the pulpal pressure satisfactorily, showed significantly lower
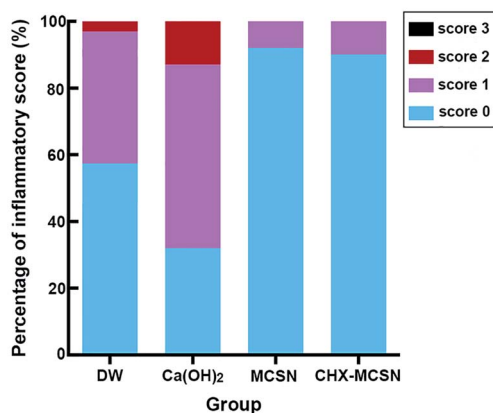

Fig. 12 Pulp inflammatory score of different groups after treatments.

dentin permeability in MCSN and CHX–MCSN groups. This result also proved MCSN-induced mineral layer could obstruct the exposed dentinal tubules well to prevent external irritants from getting deeper into the pulp.

Antibacterial and drug release results showed that MCSN could efficiently load differently-concentrated CHX, reveal significant effects against *E. faecalis*, and release the drug in a sustained way. These results showed MCSN could be used as an ideal therapeutic agent to kill the already existing bacteria in the dentinal tubes and also as a prophylactic agent to inhibit the further invasion of bacteria. These phenomena may be attributable to several reasons. First, MCSN possesses a high surface area.[42] For high surface area materials, there is great molecular retention and, as a result, a slower drug release compared with materials exhibiting smaller surface areas.[43] Second, MCSN possesses high pore size.[38] The pore size determines the available space to load molecules of the drug. The larger the pore size, the greater the drug loaded to influence the drug release.[44]

Cytotoxicity results showed that $Ca(OH)_2$ resulted in less cell viability at a concentration of 160 mg mL^{-1} and higher due to high pH and hydroxyl ions.[45] Contrarily, MCSN possessed lower cytotoxicity *in vitro* in the studied dosage range and induced ≤15% HDPC death even when the concentration reached the highest of 640 mg mL^{-1}. But when loaded with CHX, MCSN induced severe cell death when the concentration of 2%CHX–MCSN was up to 320 μg mL^{-1}. Surprisingly, histological analyses of the *in vivo* samples showed different observations. HE stain pictures showed that the blood vessels were filled with erythrocytes in the $Ca(OH)_2$ treatment group, indicating congestion and moderate inflammatory responses. But for the MCSN group and CHX–MCSN group, only a few erythrocytes were found. Further, large amounts of odontoblasts were presented in the CHX–MCSN group. Inflammatory scores were significantly lower in the two MCSN containing groups than the $Ca(OH)_2$ group. These observations suggested that CHX–MCSN did not show detrimental effects on dental pulp cells *in vivo*, even when 2%CHX was loaded on MCSN. That might be due to the effects of Ca^{2+} and SiO_3^{2-} release from CHX–MCSN and MCSN.[42] The sustained Ca^{2+} and SiO_3^{2-} release is beneficial for tissue regeneration *in vivo*.[46]

One limitation should be noted in this study. The dentin permeability *in vivo* was evaluated only for 4 days. That was because in our pilot study, we observed that the cavities prepared at the cervical region on the buccal surfaces had moved to the incisal margin due to the continuous growth of the rat incisors. Therefore, 4 days was considered to be a relatively accredited long period. Even so, in comparison with dentin hypersensitivity in human teeth can, nowadays, only being assessed by external extraction, replication, or the dentin biopsy *in vitro*, the animal model still effectively helps to study how these desensitizing agents affect the dentin *in vivo*.[47]

To the best of our knowledge, this is the first trial to apply MCSN on exposed dentin surfaces both *in vitro* and *in vivo* for detecting the occluding effect and therapy for dentin hypersensitivity. More importantly, when loaded with CHX, CHX–MCSN showed excellent remineralization, drug-delivery, and antibacterial properties *in vitro*, as well as preeminent occluding

ability *in vivo*. In consideration of these features, CHX–MCSN could be recommended as a versatile biomaterial and an appropriate agent for treating dentin hypersensitivity and inhibiting further pulp infection, which offers an optimal alternative for clinical dentists.

5. Conclusion

To sum up, MCSN could be used as a promising biomaterial for occluding the dentinal tubules *in vitro* and *in vivo* by reconstructing the enamel-like apatite layers. Also, the outstanding ability to deliver drugs and antibacterial properties enable it to carry antibiotics easily for inhibiting deeper pulp infection.

Conflicts of interest

There are no conflicts to declare.

Acknowledgements

References

1 A. G. Fincham, J. Moradian-Oldak and J. P. Simmer, The structural biology of the developing dental enamel matrix, *J. Struct. Biol.*, 1999, **126**, 270–299.

2 Y. Z. Zhou, Y. Cao, W. Liu, C. H. Chu and Q. L. Li, Polydopamine-induced tooth remineralization, *ACS Appl. Mater. Interfaces*, 2012, **4**, 6901–6910.

3 M. Goldberg, A. B. Kulkarni, M. Young and A. Boskey, Dentin: structure, composition and mineralization, *Front. Biosci.*, 2011, **3**, 711–735.

4 Y. C. Chiang, H. P. Lin, H. H. Chang, Y. W. Cheng, H. Y. Tang, W. C. Yen, P. Y. Lin, K. W. Chang and C. P. Lin, A mesoporous silica biomaterial for dental biomimetic crystallization, *ACS Nano*, 2014, **8**, 12502–12513.

5 B. Collaert and C. Fischer, Dentine hypersensitivity: a review, *Endod. Dent. Traumatol.*, 1991, **7**, 145–152.

6 G. R. Holland, M. N. Narhi, M. Addy, L. Gangarosa and R. Orchardson, Guidelines for the design and conduct of clinical trials on dentine hypersensitivity, *J. Clin. Periodontol.*, 1997, **24**, 808–813.

7 Y. Sa, Y. Gao, M. Wang, T. Wang, X. Feng, Z. Wang, Y. Wang and T. Jiang, Bioactive calcium phosphate cement with excellent injectability, mineralization capacity and drug-delivery properties for dental biomimetic reconstruction and minimum intervention therapy, *RSC Adv.*, 2016, **6**, 27349–27359.

8 N. Shoji, Y. Endo, M. Iikubo, T. Ishii, H. Harigae, J. Aida, M. Sakamoto and T. Sasano, Dentin hypersensitivity-like tooth pain seen in patients receiving steroid therapy: An exploratory study, *J. Pharmacol. Sci.*, 2016, **132**, 187–191.

9 H. J. Shiau, Dentin Hypersensitivity, *J. Evid. Based Dent. Pract.*, 2012, **12**, 220–228.

10 M. R. Bergamini, M. M. Bernardi, I. B. Sufredini, M. T. Ciaramicoli, R. M. Kodama, F. Kabadayan and C. H. Saraceni, Dentin hypersensitivity induces anxiety and increases corticosterone serum levels in rats, *Life Sci.*, 2014, **98**, 96–102.

11 M. Toledano-Osorio, E. Osorio, F. S. Aguilera, *et al.*, Improved reactive nanoparticles to treat dentin hypersensitivity, *Acta Biomater.*, 2018, **72**, 371–380.

12 S. Valimaa, L. Perea-Lowery, J. H. Smatt, *et al.*, Grit blasted aggregates of hydroxyl apatite functionalized calcium carbonate in occluding dentinal tubules, *Heliyon*, 2018, **4**(12), e01049.

13 M. Brannstrom, Dentin sensitivity and aspiration of odontoblasts, *J. Am. Dent. Assoc., JADA*, 1963, **66**, 366–370.

14 P. R. Schmidlin and P. Sahrmann, Current management of dentin hypersensitivity, *Clin. Oral Investig.*, 2013, **17**(suppl. 1), S55–S59.

15 Z. Zhou, G. Xingyun, B. Minxia, *et al.*, Remineralization of dentin slices using casein phosphopeptide–amorphous calcium phosphate combined with sodium tripolyphosphate, *Biomed. Eng.*, 2020, **19**(1), 18.

16 M. G. Mathew, A. J. Soni, M. M. Khan, *et al.*, Efficacy of remineralizing agents to occlude dentinal tubules in primary teeth subjected to dentin hypersensitivity in vitro:SEM study, *J. Family Med. Prim. Care*, 2020, **9**(1), 354–358.

17 F. Shafiei and M. Memarpour, Antibacterial activity in adhesive dentistry: a literature review, *Gen. Dent.*, 2012, **60**, e346–e356, quiz e357–e358.

18 P. N. De Aza, F. Guitian and S. De Aza, Bioeutectic: a new ceramic material for human bone replacement, *Biomaterials*, 1997, **18**, 1285–1291.

19 W. Xue, X. Liu, X. Zheng and C. Ding, In vivo evaluation of plasma-sprayed wollastonite coating, *Biomaterials*, 2005, **26**, 3455–3460.

20 L. Fei, C. Wang, Y. Xue, K. Lin, J. Chang and J. Sun, Osteogenic differentiation of osteoblasts induced by calcium silicate and calcium silicate/beta-tricalcium phosphate composite bioceramics, *J. Biomed. Mater. Res., Part B*, 2012, **100**, 1237–1244.

21 Y. Zhu, M. Zhu, X. He, J. Zhang and C. Tao, Substitutions of strontium in mesoporous calcium silicate and their physicochemical and biological properties, *Acta Biomater.*, 2013, **9**, 6723–6731.

22 C. Wu, J. Chang and W. Fan, Bioactive mesoporous calcium-silicate nanoparticles with excellent mineralization ability, osteostimulation, drug-delivery and antibacterial properties for filling apex roots of teeth, *J. Mater. Chem.*, 2012, **22**, 16801.

23 X. Li, J. Shi, Y. Zhu, W. Shen, H. Li, J. Liang and J. Gao, A template route to the preparation of mesoporous amorphous calcium silicate with high in vitro bone-forming bioactivity, *J. Biomed. Mater. Res., Part B*, 2007, **83**, 431–439.

24 G. Wei and P. X. Ma, Nanostructured Biomaterials for Regeneration, *Adv. Funct. Mater.*, 2008, **18**, 3566–3582.

25 M. Schumacher, L. Reither, J. Thomas, M. Kampschulte, U. Gbureck, A. Lode and M. Gelinsky, Calcium phosphate bone cement/mesoporous bioactive glass composites for controlled growth factor delivery, *Biomater. Sci.*, 2017, **5**, 578–588.

26 Y. Wang, Q. Zhao, N. Han, L. Bai, J. Li, J. Liu, E. Che, L. Hu, Q. Zhang, T. Jiang and S. Wang, Mesoporous silica nanoparticles in drug delivery and biomedical applications, *Nanomedicine*, 2015, **11**, 313–327.

27 J. Wei, F. Chen, J. W. Shin, H. Hong, C. Dai, J. Su and C. Liu, Preparation and characterization of bioactive mesoporous wollastonite – polycaprolactone composite scaffold, *Biomaterials*, 2009, **30**, 1080–1088.

28 Y. Li, N. Li, W. Pan, Z. Yu, L. Yang and B. Tang, Hollow Mesoporous Silica Nanoparticles with Tunable Structures for Controlled Drug Delivery, *ACS Appl. Mater. Interfaces*, 2017, **9**, 2123–2129.

29 W. Xue, A. Bandyopadhyay and S. Bose, Mesoporous calcium silicate for controlled release of bovine serum albumin protein, *Acta Biomater.*, 2009, **5**, 1686–1696.

30 X. Kang, S. Huang, P. Yang, P. Ma, D. Yang and J. Lin, Preparation of luminescent and mesoporous Eu^{3+}/Tb^{3+} doped calcium silicate microspheres as drug carriers via a template route, *Dalton Trans.*, 2011, **40**, 1873–1879.

31 X. Liu, N. Zhang, Y. Yao, H. Sun and H. Feng, Micro-structural characterization of the hydration products of bauxite-calcination-method red mud-coal gangue based cementitious materials, *J. Hazard. Mater.*, 2013, **262**, 428–438.

32 L. Han and T. Okiji, Bioactivity evaluation of three calcium silicate-based endodontic materials, *Int. Endod. J.*, 2013, **46**, 808–814.

33 P. N. De Aza, J. E. Mate-Sanchez de Val, C. Baudin, C. Perez Albacete-Martinez, A. Armijo Salto and J. L. Calvo-Guirado, Bone neoformation of a novel porous resorbable Si–Ca–P-based ceramic with osteoconductive properties: physical and mechanical characterization, histological and histomorphometric study, *Clin. Oral Implants Res.*, 2016, **27**, 1368–1375.

34 N. Schlueter, M. Hardt, A. Lussi, F. Engelmann, J. Klimek and C. Ganss, Tin-containing fluoride solutions as anti-erosive agents in enamel: an in vitro tin-uptake, tissue-loss, and scanning electron micrograph study, *Eur. J. Oral Sci.*, 2009, **117**, 427–434.

35 D. S. Kim, J. Kim, K. K. Choi and S. Y. Kim, The influence of chlorhexidine on the remineralization of demineralized dentine, *J. Dent.*, 2011, **39**, 855–862.

36 S. Jenkins, M. Addy and W. Wade, The mechanism of action of chlorhexidine. A study of plaque growth on enamel inserts in vivo, *J. Clin. Periodontol.*, 1988, **15**, 415–424.

37 A. C. Romano, A. C. Aranha, B. L. da Silveira, S. L. Baldochi and P. Eduardo Cde, Evaluation of carbon dioxide laser irradiation associated with calcium hydroxide in the treatment of dentinal hypersensitivity. A preliminary study, *Lasers Med. Sci.*, 2011, **26**, 35–42.

38 W. Fan, D. Wu, F. R. Tay, T. Ma, Y. Wu and B. Fan, Effects of adsorbed and templated nanosilver in mesoporous calcium-

silicate nanoparticles on inhibition of bacteria colonization of dentin, *Int. J. Nanomed.*, 2014, **9**, 5217–5230.

39 K. J. Heyeraas, O. B. Sveen and I. A. Mjor, Pulp–dentin biology in restorative dentistry. Part 3: pulpal inflammation and its sequelae, *Quintessence International*, 2001, **32**, 611–625.

40 T. Jiang, X. Ma, Y. Wang, Z. Zhu, H. Tong and J. Hu, Effects of hydrogen peroxide on human dentin structure, *J. Dent. Res.*, 2007, **86**, 1040–1045.

41 S. G. Kazarian and K. L. Chan, Applications of ATR-FTIR spectroscopic imaging to biomedical samples, *Biochim. Biophys. Acta*, 2006, **1758**, 858–867.

42 W. Fan, Y. Li, Q. Sun, T. Ma and B. Fan, Calcium-silicate mesoporous nanoparticles loaded with chlorhexidine for both anti-*Enterococcus faecalis* and mineralization properties, *J. Nanobiotechnol.*, 2016, **14**, 72.

43 A. L. Doadrio, A. J. Salinas, J. M. Sanchez-Montero and M. Vallet-Regi, Drug release from ordered mesoporous silicas, *Curr. Pharm. Des.*, 2015, **21**, 6213–6819.

44 M. Vallet-Regí, F. Balas, M. Colilla and M. Manzano, Bone-regenerative bioceramic implants with drug and protein controlled delivery capability, *Prog. Solid State Chem.*, 2008, **36**, 163–191.

45 M. Zare Jahromi, P. Ranjbarian and S. Shiravi, Cytotoxicity evaluation of Iranian propolis and calcium hydroxide on dental pulp fibroblasts, *J. Dent. Res. Dent. Clin. Dent. Prospects*, 2014, **8**, 130–133.

46 X. Wang, Y. Zhou, L. Xia, C. Zhao, L. Chen, D. Yi, J. Chang, L. Huang, X. Zheng, H. Zhu, Y. Xie, Y. Xu and K. Lin, Fabrication of nano-structured calcium silicate coatings with enhanced stability, bioactivity and osteogenic and angiogenic activity, *Colloids Surf., B*, 2015, **126**, 358–366.

47 D. H. El Rouby, M. H. Bashir and N. S. Korany, The effect of lathyrism on dentin structure of the rat incisors: a morphometric and scanning electron microscopic investigation, *J. Oral Pathol. Med.*, 2010, **39**, 424–430.